NMR determination of order parameters in the quadrupolar glasses $Na(CN)_xCl_{1-x}$ and $Na_xK_{1-x}CN$

W. Wiotte and J. Petersson
Fachbereich Physik, Universität des Saarlandes, D-6600 Saarbrücken, Federal Republic of Germany

R. Blinc
J. Stefan Institute, E. Kardely University of Ljubljana, Ljubljana, Yugoslavia

S. Elschner*
Fachbereich Physik, Universität des Saarlandes, D-6600 Saarbrücken, Federal Republic of Germany
(Received 25 September 1990)

It is shown that quadrupolar perturbed nuclear magnetic resonance (NMR) is a powerful method to investigate the quadrupolar glasses $Na(CN)_xCl_{1-x}$ and $Na_xK_{1-x}CN$. In both systems at the sodium and chlorine sites, distributions of electric-field-gradient tensors occur which are restricted by the fact that the average structure of the systems under investigation is cubic. Correspondingly, inhomogeneous distributions of NMR lines result, which for $I=\frac{3}{2}$ nuclear-spin systems consist of inhomogeneously broadened central lines and broad distributions of satellite lines. Measurements of these frequency distributions and their dependences on the composition, the orientation, and the temperature of the samples are presented. The widths of the electric-field-gradient-tensor distributions are related in a general quadrupolar glass model to the quadrupolar Edwards-Anderson order parameter q_{EA}. As a consequence, the temperature dependence of q_{EA} is derived, reflecting the random orientational freeze-out of the CN quadrupoles with decreasing temperature. By interpreting the results in terms of theoretical models, it is shown that in the mixed cyanides we deal with a smearing of a collective quadrupolar glass transition by weak random fields and not with a pure random-field-type freezing or a pure random-bond-type glass transition. The results are compared to those obtained from other experimental methods. In particular, the critical elastic behavior of these systems is discussed in a general context.

I. INTRODUCTION

Several insulating mixed systems containing molecular groups show a glassy behavior at low temperatures over a certain range of composition. Well-known examples which have been thoroughly investigated by various experimental methods in recent years are the dipolar glasses $Rb_x(NH_4)_{1-x}H_2PO_4$ (RADP) (Refs. 1 and 2) and $KTaO_3$:Li (Ref. 3) and the quadrupolar glasses of the types $M(CN)_xX_{1-x}$ (Refs. 4–7) and $M_xM'_{1-x}CN$,[8–11] where X is a halide ion and M and M' denote alkali-metal ions. The great interest which has been devoted particularly to the latter systems is caused by the fact that they show, in certain concentration ranges, a great variety of structural phase transitions, whereas for other concentration ranges they are considered as model systems for quadrupolar (or "orientational") glasses. These different features are brought about by the dumbbell-shaped CN ions forming elastic quadrupoles, whose strain-mediated interactions determine the anomalous static and dynamic properties.

Quadrupolar glasses[12,13] may form a conceptual link between spin glasses[14]—where, for certain models, exact solutions[15,16] exist demonstrating a phase transition to another thermodynamic state—and conventional glasses which are much less understood and whose behavior is generally believed[17,18] to be dominated by metastable states. The quadrupolar glasses of the type discussed here are characterized by a random orientational freeze-out of the molecular quadrupoles, i.e., the dumbbell-shaped CN groups in the mixed cyanides,[7,19–24] without any head-tail (i.e., dipolar) ordering. This is to be compared with the random head-tail freeze-out of the Ising spins in a classical spin glass. In both cases, the freeze-out is driven by randomly frustrated competing interactions. The quadrupolar glass, however, is more subtle and more complex. In spin glasses the competing interactions are individually deterministic, i.e., each individual interaction demands a unique—ferromagnetic or antiferromagnetic—ordering of the spins it connects. In quadrupolar glasses, on the other hand, the interactions are not equally definite and permit a greater variety of choices. Thus, the pattern of orientations which the axes of the CN dumbbells take at low temperatures is principally, i.e., even in an ideal mixed system, not uniquely determined and reflects the influence of frustration and disorder on the transition to the glass state. Another important feature is the dominating coupling of the orientational degrees of freedom of the CN molecules to elastic lattice waves[19–21] giving rise to an enormous softening of the elastic shear modulus c_{44} (Refs. 7 and 25–29) reflecting—at least in certain concentration ranges— the

collective properties of the transition to the glass state. Moreover, the substitutional disorder results in local random strain fields at the sites of the CN molecules. Analogous effects are unimportant in magnetic spin glasses.

As model systems for quadrupolar glasses, we studied the mixed alkali cyanides $Na(CN)_xCl_{1-x}$ (Refs. 7, 24, and 30) and $Na_xK_{1-x}CN$.[8,10,31] The $Na(CN)_xCl_{1-x}$ (Ref. 30) system [see Fig. 1(a)] shows, for high CN concentrations, ferroelastic phase transitions from an orientationally disordered cubic phase to rhombohedral or orthorhombic phases where the CN groups are orientationally ordered but can still perform 180° head-tail flips. Below a critical concentration x_c, no such macroscopic phase transitions exist[30] and the system remains, on the average, cubic down to lowest temperatures. Nevertheless, an orientational freezing of the CN quadrupoles occurs, resulting in a quadrupolar glass state. In the $Na_xK_{1-x}CN$ system [see Fig. 1(b)], the structural phase transitions are observed only for compositions close to those of the pure compounds NaCN and KCN,[8,10] which undergo an identical sequence of structural phases with, of course, different transition temperatures. For $0.1 \lesssim x \lesssim 0.85$, the phase transition is suppressed[8] and a quadrupolar glass state occurs.

It will be shown that quadrupolar perturbed nuclear magnetic resonance (NMR) is a powerful and sensitive experimental tool for investigating the glass transitions in these systems. Predominantly, the ^{23}Na nucleus and, in some cases, the ^{35}Cl nucleus were investigated. Both nuclei have the spin $I=\frac{3}{2}$ and therefore the interaction between the electric-field-gradient (EFG) tensor at the nucleus and the quadrupole moment of the nucleus results in a—in some cases, considerable—perturbation of the Zeeman levels of the nuclear spin system. It is well known that, as a consequence, in first-order perturbation calculation, the spectrum of the NMR lines at any nucleus consists of an unshifted central line ($m=\frac{1}{2} \leftrightarrow m=-\frac{1}{2}$) at the Larmor frequency ν_L and two satellite lines ($m=\pm\frac{1}{2} \leftrightarrow m=\pm\frac{3}{2}$) shifted from ν_L by the same amount to higher and lower frequencies. In second-order perturbation calculation, all lines are shifted in the way that the distance of the satellites is still a pure first-order effect. It is one of the purposes of this contribution to present experimental results concerning the distributions of both central and satellite lines in the mixed cyanides $Na(CN)_xCl_{1-x}$ and $Na_xK_{1-x}CN$ and their dependences on parameters as, e.g., the composition (degree of disorder), the orientation, and the temperature of the samples.

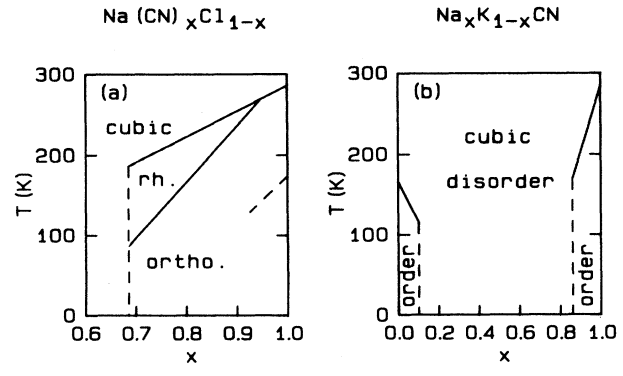

FIG. 1. Schematic representation of the phase diagrams of (a) the $Na(CN)_xCl_{1-x}$ system (rh ≅ rhombohedral, ortho ≅ orthorhombic; after Ref. 7) and (b) the $Na_xK_{1-x}CN$ system (after Ref. 8; for more particulars see Ref. 10).

In spite of many investigations,[7,19–32] the nature of the observed random orientational freeze-out in the mixed cyanides is still not clear. One of the main questions is whether there is a true collective transition driven by randomly frustrated competing interactions occurring at a nonzero transition temperature T_g or just a strong random-field-type single-ion freezing with the local random fields determining the alignment of the orientational degrees of freedom.[32,33] The solution of this question is complicated by the fact that the Edwards-Anderson order parameter q_{EA} characterizing the spin glass as well as the quadrupolar glass state has no macroscopic conjugate field and is therefore hard to measure directly. We will show that quadrupolar perturbed NMR renders it possible to determine the Edwards-Anderson order parameter q_{EA} and, thus, can contribute to resolve this problem.

The paper is organized as follows: In Sec. II some experimental details are briefly described. In Sec. III the distributions of EFG's and NMR frequencies in an average cubic structure will be discussed in a general context. Section IV will be devoted to the presentation of the results of our NMR measurements in the systems $Na(CN)_xCl_{1-x}$ and $Na_xK_{1-x}CN$. In Sec. V, a theoretical model for quadrupolar glasses will be developed. Starting from the definition of order parameters, the Edwards-Anderson order parameter q_{EA} will be related to the measured second moment of the EFG tensor distributions reflecting the degree of orientational freezing of the CN ions. In Sec. VI, the temperature dependence of q_{EA} will be derived from the measured temperature dependences of the EFG distributions and related to the predictions of theoretical models. Finally (Sec. VII), the results are compared to those obtained from other experimental methods discussing, in particular, the relation to the elastic behavior.

II. EXPERIMENTAL DETAILS

In our experiments, single crystals of $Na(CN)_xCl_{1-x}$ and $Na_xK_{1-x}CN$ were used, which were grown from the melt. Details of the crystal-growth procedure are described in Ref. 34. For the case of the $Na(CN)_xCl_{1-x}$ system, the concentration x, given in the following, refers to the composition of the sample under investigation determined by the methods described previously.[34] For the case of the $Na_xK_{1-x}CN$ system, x refers to the composition of the melt. It was shown recently by space-resolving Brillouin-scattering studies of the elastic shear stiffness c_{44} (Refs. 34 and 35) that, as a general consequence of the crystal-growth technique, significant spatial concentration gradients of about 2%/cm exist in every direction of the samples. As in our NMR experiments, samples with rather big volumes of about 1 cm^3 are used,

we principally measure an integral over an inhomogeneous sample. Since the concentration variations in every sample are small compared to the concentration differences between different samples and because of the limited measuring accuracy and resolution, this effect is unimportant in the present context.

We employed a Bruker CXP 300 NMR pulse spectrometer operating with a superconducting magnet with a static magnetic field of 7.046 T. In addition, using a conventional electromagnet, shapes of the ^{23}Na central lines were measured at static magnetic fields of 0.488 and 1.772 T. The shapes of the ^{23}Na and ^{35}Cl central lines were obtained both from the free induction decay (FID) and from the echo following a 90°-τ-90° pulse sequence. Because of their considerable widths, the distributions of the ^{23}Na satellites were determined by applying a hole-burning technique: the durations of the pulses (usually about 100 μs) of a 90°-τ-90° sequence were chosen in such a way that only a small slice of the spectrum was irradiated. For any chosen frequency, about 4000 scans had to be used at a repetition rate of about 0.1 s. The distribution function of the satellite frequencies is then given by the frequency dependence of the intensity of the signal obtained by Fourier transforming the decay of the occurring echo.

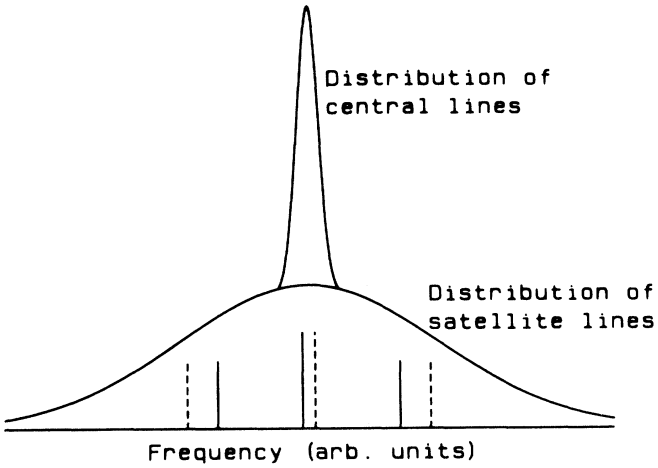

FIG. 2. Schematic representation of the NMR frequency distributions of $I=\frac{3}{2}$ nuclei caused by EFG distributions. Solid lines and dotted lines indicate schematically the line spectra of two nuclei with different EFG's.

III. DISTRIBUTIONS OF EFG'S AND NMR FREQUENCIES

In pure NaCl, as well as in the high-temperature phase of pure NaCN, the EFG at the ^{23}Na nucleus vanishes as a consequence of cubic symmetry. Mixed systems $Na(CN)_xCl_{1-x}$ and $Na_xK_{1-x}CN$, which do not undergo a phase transition, stay cubic down to lowest temperatures. The local surroundings of the ^{23}Na and ^{35}Cl nuclei in these systems, however, in general, deviate from the cubic symmetry and thus an EFG occurs. Due to the distribution of local surroundings, a distribution of EFG's is expected, leading to an inhomogeneous broadening of the central line and a wide spread of satellite transitions. This fact is schematically depicted in Fig. 2.

In the following, the restrictions will be formulated which are imposed on the distribution functions of the EFG components and, consequently, of the NMR frequencies by the fact that the average crystal structure is cubic. The results to be presented may be considered as extensions of those of Refs. 24 and 36.

In a Cartesian laboratory reference frame (x,y,z) with the static magnetic field $\mathbf{B}_0$ directed along the z axis, the first-order shift $\nu_i^{(1)}$ of the satellites and the second-order shift $\nu_i^{(2)}$ of the central line, respectively, at a nucleus (spin $I=\frac{3}{2}$) located at site i are given by[37]

$$\nu_i^{(1)}=\pm\frac{K}{2}V_{zz}^i \ , \tag{1}$$

$$\nu_i^{(2)}=\frac{K^2}{12\nu_L}\{\tfrac{1}{4}(V_{xx}^i-V_{yy}^i)^2+(V_{xy}^i)^2 -2[(V_{xz}^i)^2+(V_{yz}^i)^2]\} \ . \tag{2}$$

Here, $V_{mn}^i=\partial^2V/\partial x_m\partial x_n$ denotes the EFG at the site of the nucleus, $K=eQ/h$ and eQ is the electric quadrupole moment of the nucleus. Thus, first-order effects probe one component of the EFG tensor, whereas the second-order shift of the central line is a quadratic effect generally determined by several EFG tensor elements.

At each nuclear site, the EFG tensor elements may be expressed in a reference frame whose Cartesian axes a,b,c are directed along the cubic axes of the average cubic structure. Because of the disorder in the system, these elements $V_{\alpha\beta}$, where α and $\beta=a,b,c$, are distributed according to some distribution functions. As a consequence of the validity of the Laplace condition $V_{aa}+V_{bb}+V_{cc}=0$ for each individual EFG, it suffices to consider, for the main diagonal elements, the combined distribution function $p(V_{aa},V_{bb})$ which, because of the average cubic structure, obeys the relation

$$p(V_{aa},V_{bb})=p(V_{bb},V_{cc})=p(V_{aa},V_{cc}) \ . \tag{3}$$

Due to the average cubic structure, the distribution functions for the individual main diagonal elements are identical:

$$p(V_{aa})=p(V_{bb})=p(V_{cc}) \ . \tag{4}$$

These distribution functions are related to those in (3) in the usual way by

$$p(V_{\alpha\alpha})=\int p(V_{\alpha\alpha},V_{\beta\beta})dV_{\beta\beta}, \quad \alpha\neq\beta \ . \tag{5}$$

A relation analogous to (4) holds for the distribution functions for the off-diagonal elements:

$$p(V_{ab})=p(V_{ac})=p(V_{bc}) \ . \tag{6}$$

Contrary to the main diagonal elements, there exists no *a priori* restriction for the off-diagonal elements at each individual site. Thus, the off-diagonal elements are assumed to be independently distributed. As a consequence, relations of the type

$$p(V_{ab},V_{ac})=p(V_{ab})p(V_{ac}) \tag{7}$$

hold. Because of the average cubic structure, the distribution functions in Eqs. (4) and (6) are even functions of the respective variables. Consequently, their first moments, defined as usual by

$$[V_{\alpha\beta}]_{\rm av}=\int V_{\alpha\beta}p(V_{\alpha\beta})dV_{\alpha\beta}\ , \tag{8a}$$

vanish, i.e., the mean EFG vanishes. For the second moments, defined as usual by

$$[V^2_{\alpha\beta}]_{\rm av}=\int V^2_{\alpha\beta}p(V_{\alpha\beta})dV_{\alpha\beta}\ , \tag{8b}$$

the relations hold:

$$[V^2_{aa}]_{\rm av}=[V^2_{bb}]_{\rm av}=[V^2_{cc}]_{\rm av}\ , \tag{9}$$

$$[V^2_{ab}]_{\rm av}=[V^2_{bc}]_{\rm av}=[V^2_{ac}]_{\rm av}\ . \tag{10}$$

Accordingly, $[\cdots]_{\rm av}$ is an ensemble (disorder) average. Thus, for an average cubic structure, two independent second moments of the EFG components, $[V^2_{aa}]_{\rm av}$ and $[V^2_{ab}]_{\rm av}$, exist. Both quantities are a measure for the mean deviation from the cubic symmetry.

The distribution of NMR resonance frequencies is thus given by

$$I(\nu)=\int p(V_{aa},V_{bb})p(V_{ab})p(V_{bc})p(V_{ac})\times\delta[\nu-\nu'(V_{aa},V_{bb},V_{ab},V_{bc},V_{ac},\Omega)]\times dV_{aa}dV_{bb}dV_{ab}dV_{bc}dV_{ac}\ , \tag{11}$$

where ν' has to be identified with $\nu^{(1)}$ or $\nu^{(2)}$ in Eqs. (1) and (2) for first- and second-order shifts, respectively, and Ω denotes, in the most general case, two angles specifying the orientation of the sample. The distribution given in (11) can only be evaluated analytically in few cases. Some of them will be discussed in the following.

In our NMR experiments, the crystal is rotated around one of the axes a,b,c of the average cubic structure. Thus, the static magnetic field $\mathbf{B}_0$ lies in a plane orthogonal to that axis, e.g., the a axis, and the crystal orientation can be specified by the angle φ between the direction of $\mathbf{B}_0$ and one crystallographic axis, e.g., the b axis, being orthogonal to the rotation axis. The following discussion is therefore restricted to this case. In the laboratory reference frame, the symmetric EFG tensor can then be expressed as

$$(V_{mn})=\begin{bmatrix} V_{aa} & V_{ab}\cos\varphi+V_{ac}\sin\varphi & -V_{ab}\sin\varphi+V_{ac}\cos\varphi \\ V_{ab}\cos\varphi+V_{ac}\sin\varphi & V_{bb}\cos^2\varphi+V_{cc}\sin^2\varphi+V_{bc}\sin2\varphi & \frac{1}{2}(V_{cc}-V_{bb})\sin2\varphi+V_{bc}\cos2\varphi \\ -V_{ab}\sin\varphi+V_{ac}\cos\varphi & \frac{1}{2}(V_{cc}-V_{bb})\sin2\varphi+V_{bc}\cos2\varphi & V_{bb}\sin^2\varphi+V_{cc}\cos^2\varphi-V_{bc}\sin2\varphi \end{bmatrix}\ . \tag{12}$$

First of all, the distribution of satellite lines will be investigated. For any crystal orientation just specified, the second moment

$$M_2^{(1)}=[(\nu_i^{(1)})^2]_{\rm av}$$

of this distribution can now be calculated without further restrictions. Taking into account (1), (12), and the average cubic structure—then, e.g., (9), (10), and

$$2[V_{aa}V_{bb}]_{\rm av}=-[V^2_{aa}]_{\rm av}$$

hold—$M_2^{(1)}(\varphi)$ is given by

$$M_2^{(1)}(\varphi)=\frac{K^2}{4}\{[V^2_{aa}]_{\rm av}[1-\tfrac{3}{4}\sin^2(2\varphi)]+[V^2_{ab}]_{\rm av}\sin^2(2\varphi)\}\ . \tag{13}$$

Thus, from a measurement of the orientational dependence of the second moment of this distribution, the second moments $[V^2_{aa}]_{\rm av}$ and $[V^2_{ab}]_{\rm av}$ of the distributions of the main diagonal and of the off-diagonal elements, respectively, of the EFG tensors at the sites of the nuclei are obtained. [According to (1), the distribution function of the satellites is symmetric, i.e., the first moment $M_1^{(1)}$ of this distribution vanishes.]

The shapes of the distributions of the satellite frequencies measured for most cases in the mixed cyanides justify, for any crystal orientation just specified, the assumption of a Gaussian distribution function for the satellite lines

$$I^{(1)}(\nu)=[2\pi M_2^{(1)}(\varphi)]^{-1/2}\exp\left[-\frac{\nu^2}{2M_2^{(1)}(\varphi)}\right]\ , \tag{14}$$

with $M_2^{(1)}(\varphi)$ from Eq. (13). Gaussian distributions of this type have been derived already by Cohen and Reif,[36] who calculated the frequency distributions for the satellite lines and the central line in an imperfect cubic crystal assuming that the distribution of defects is completely random and that each nucleus is perturbed by a sufficient number of sites. Thus, the occurrence of Gaussian distributions for the satellites is a consequence of the central-limit theorem.

Note the general validity of Eq. (13) for $M_2^{(1)}(\varphi)$. Its applicability is not restricted to the case of Gaussian distributions. Thus, it can, in principle also be applied to the more general case observed in some mixed alkali cyanides at low temperatures where deviations from the Gaussian laws become important. The practical determination of the second moment from the experimental data is simple for Gaussian distributions, whereas it is rather difficult for distributions of arbitrary shape.

With respect to (14), (normalized) Gaussian distributions for the different EFG components may be reasonably assumed:

$$p(V_{aa},V_{bb})=\frac{\sqrt{3}}{2\pi b^2}\exp\left[-\frac{V_{aa}^2+V_{bb}^2+V_{aa}V_{bb}}{b^2}\right], \quad (15a)$$

$$p(V_{aa})=\frac{1}{\sqrt{2\pi}a}\exp\left[-\frac{V_{aa}^2}{2a^2}\right], \quad (15b)$$

and

$$p(V_{ab})=\frac{1}{\sqrt{2\pi}c}\exp\left[-\frac{V_{ab}^2}{2c^2}\right], \quad (15c)$$

where $[V_{aa}^2]_{\rm av}=a^2$, $[V_{ab}^2]_{\rm av}=c^2$, and because of (5), $a^2=2b^2/3$. The quadratic form occurring in the exponent of Eq. (15a) can be written in diagonal form by transforming to the variables $V_{aa}+V_{bb}$ and $V_{aa}-V_{bb}$. Taking into account the Laplace condition, the validity of condition (3) can be easily proved. Equations (13) and (14) can be directly derived by substituting (15) in (11).

The derivation of corresponding general expressions for the distribution of central lines is rather complicated. Substituting (12) in (2) and assuming again an average cubic structure, the first moment

$$M_1^{(2)}(\varphi)=[\nu_i^{(2)}]_{\rm av},$$

i.e., the shift, of the central line can be calculated for the crystal orientation specified above

$$M_1^{(2)}(\varphi)=\frac{K^2}{4\nu_L}\{\tfrac{1}{4}[V_{aa}^2]_{\rm av}[1-\tfrac{9}{4}\sin^2(2\varphi)] +[V_{ab}^2]_{\rm av}[\tfrac{3}{4}\sin^2(2\varphi)-1]\}. \quad (16)$$

A general calculation of the second moment $M_2^{(2)}(\varphi)$ of the central line distribution according to (12) and (2) results in a complicated analytical relationship. Since its practical applicability to the present case is restricted by the limited experimental accuracy and, moreover, by the fact that the dipolar linewidth has to be taken into account on evaluating the data, this analytical expression is not presented here.

The calculation of the frequency distribution of the central line according to (11) constitutes another more complicated problem. Special results for $I(\nu)$ are given in previous works for the following cases: (i) for a general EFG and $\mathbf{B}_0\|[100]$, an analytical expression holds for $\nu<0$, whereas, for $\nu>0$, an integral is derived,[36] (ii) for $[V_{ab}^2]_{\rm av}=0$ and a crystal orientation specified by the angle φ, Elschner *et al.*[24] used (15a) to calculate, according to (11), the analytical form of $I(\nu)$. As will be shown below, for the mixed alkali cyanides, the latter case $[V_{ab}^2]_{\rm av}=0$ is realized to a good approximation. This means that $V_{ab}=V_{bc}=V_{ac}=0$, i.e., the principal axes of the EFG at each nucleus are directed along the directions of the axes of the average cubic structure.

The relations (3)–(13) and (16) generally hold for an average cubic structure. Therefore, in particular, the case is included that a given EFG with the principal components V_{11}, V_{22}, and V_{33} is randomly distributed over all orientations. The corresponding NMR frequency distributions are well known (powder spectrum).[36] Here, we only want to note that, for this case,

$$[V_{aa}^2]_{\rm av}=\tfrac{2}{15}(V_{11}^2+V_{22}^2+V_{33}^2)$$

and

$$[V_{ab}^2]_{\rm av}=\tfrac{1}{10}(V_{11}^2+V_{22}^2+V_{33}^2).$$

Consequently, $3[V_{aa}^2]_{\rm av}=4[V_{ab}^2]_{\rm av}$. Therefore, as expected, both the distribution of satellite lines (13) and the shift of the central line (16) do not depend on the crystal orientation.

It is worthwhile comparing the present case of an EFG in an average cubic structure to that of the EFG at the rubidium site in the dipolar glass state of RADP.[38] In both cases, the EFG's are distributed according to Gaussian laws around the respective mean values, which are related to the mean crystal structure. For RADP, the average structure is tetragonal and it can therefore be assumed that small deviations from the large mean EFG are present. Consequently, suitable truncated expansions can be used. In the present case, on the other hand, the average structure is cubic, and thus the mean EFG vanishes. Truncated expansions are, in this case, of course, not adequate. In both cases, the deviations from the mean value are restricted by symmetry arguments.

IV. EXPERIMENTAL RESULTS

Typical experimental results obtained for the orientational dependences of the shape of the ^{23}Na central line and the distribution of the ^{23}Na satellite lines measured at a $Na_xK_{1-x}CN$ crystal with $x=0.7$ are shown in Figs. 3 and 4. Analogous results for the $Na(CN)_xCl_{1-x}$ system were presented previously in Ref. 24 and will be discussed below in a common context. Figures 3 and 4 demonstrate a distinct dependence of the spectra on the crystal orientation.

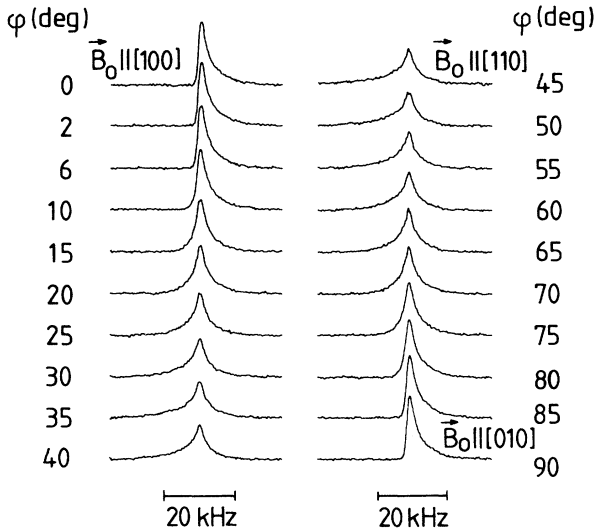

FIG. 3. Dependence of the shape of the ^{23}Na central line for a $Na_{0.7}K_{0.3}CN$ crystal on the crystal orientation specified by the angle φ as measured at $\nu_L=19.96$ MHz and $T\approx280$ K by Fourier transforming the echo. The spectra are normalized.

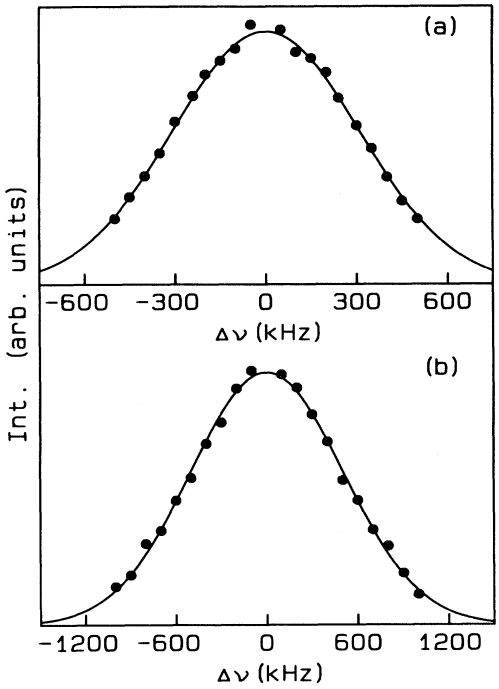

FIG. 4. Distributions of ^{23}Na satellite lines for a $Na_{0.7}K_{0.3}CN$ crystal at $\nu_L = 79.4$ MHz and $T \approx 280$ K at the crystal orientations (a) $\mathbf{B}_0 \| [110]$ and (b) $\mathbf{B}_0 \| [100]$. Note that the frequency scales differ by a factor of 2. The curves are fits to Gaussian distributions with the second moments (a) $M_2^{(1)} = 0.095$ MHz^2 and (b) $M_2^{(1)} = 0.25$ MHz^2.

As expected for an average cubic structure, the spectra in Fig. 3 show a mirror symmetry with respect to the crystal orientation $\varphi = 45°$. In particular, identical spectra are obtained for $\mathbf{B}_0$ parallel to the cubic directions. For these particular orientations, the spectra are highly asymmetric: Within the limits of experimental accuracy, only second-order shifts to higher frequencies occur. For other orientations, the spectra are less asymmetric. Figure 4 demonstrates that, at ambient temperature, the distributions of the satellite lines can be well represented by Gaussian laws whose widths depend on the crystal orientation. The frequency scales in Fig. 4 have been chosen in such a way that, for a crystal which fulfills the condition $[V_{ab}^2]_{\rm av} = 0$, the distribution functions in Figs. 4(a) and 4(b) should apparently coincide [compare to (13), (14)]. This is obviously not the case. The difference, however, is small.

In order to check the validity of (13) and (14) for the present case, we measured the orientational dependence of $M_2^{(1)}$ for $Na_xK_{1-x}CN$ crystals with the concentrations $x = 0.70$ and 0.57 at ambient temperature. The result for $Na_{0.7}K_{0.3}CN$ is presented in Fig. 5. A fit according to Eq. (13) yields the values

$$\frac{K^2}{4}[V_{aa}^2]_{\rm av} = 0.227 \text{ MHz}^2$$

and

$$\frac{K^2}{4}[V_{ab}^2]_{\rm av} = 0.011 \text{ MHz}^2 .$$

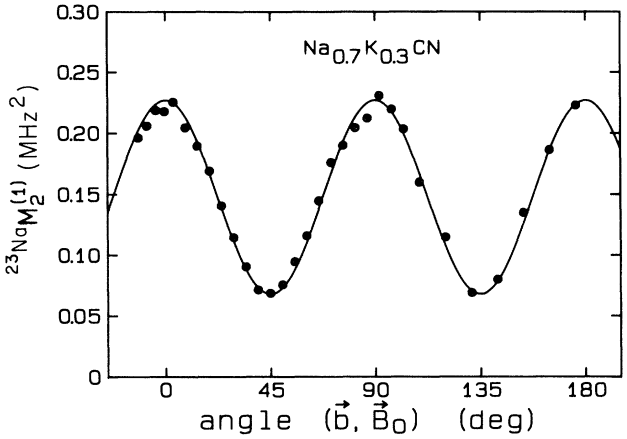

FIG. 5. Dependence of the second moment $M_2^{(1)}$ of the Gaussian ^{23}Na satellite distribution for a $Na_{0.7}K_{0.3}CN$ crystal on the crystal orientation as measured at $\mathbf{a} \perp \mathbf{B}_0$, $\nu_L = 79.4$ MHz, and $T \approx 300$ K. The curve shows a fit according to Eq. (13) with $(K^2/4)[V_{aa}^2]_{\rm av} = 0.227$ MHz^2 and $(K^2/4)[V_{ab}^2]_{\rm av} = 0.011$ MHz^2.

Note that the results in Figs. 4 and 5 do not correspond to exactly the same fit parameters because $M_2^{(1)}$ depends on the temperature (see below) and the measuring temperatures differ by about 20 K. The fit parameters for $Na_{0.57}K_{0.43}CN$ are

$$\frac{K^2}{4}[V_{aa}^2]_{\rm av} = 0.398 \text{ MHz}^2$$

and

$$\frac{K^2}{4}[V_{ab}^2]_{\rm av} = 0.006 \text{ MHz}^2 .$$

For both systems, the second moments of the distributions of the off-diagonal elements are small compared to those of the main diagonal elements. The corresponding ratios $[V_{ab}^2]_{\rm av}/[V_{aa}^2]_{\rm av}$ are 0.048 and 0.015, respectively. Thus, at each sodium site in the cubic crystal reference frame, the off-diagonal elements of the EFG tensors are small at ambient temperature. This result is equivalent to the fact that, at any sodium site, the principal axes of the EFG are essentially directed along the axes a, b, c of the average cubic structure.

A further confirmation of this statement is provided by the shapes of the central line (Fig. 3): If the crystal is orientated in a way that one crystal axis is parallel to the static magnetic field $\mathbf{B}_0$, the observed line shapes suggest that, in this orientation, the second-order shifts $\nu^{(2)}$ in (2) are positive for all nuclei. This is just equivalent to the statement $[V_{ab}^2]_{\rm av} = 0$.

Similar results were derived previously for the system $Na(CN)_xCl_{1-x}$, where $x \approx 0.65$ is near the critical concentration x_c.[24] These data were evaluated on the assumption that $[V_{ab}^2]_{\rm av} = 0$, which was derived from a behavior of the ^{23}Na central line similar to that given for the present case in Fig. 3. A closer inspection of the previous satellite distributions for $\varphi = 0$ and 45° renders it possible to estimate for $T \approx 270$ K,

$$\frac{K^2}{4}[V_{aa}^2]_{\mathrm{av}}=0.015\ \mathrm{MHz}^2$$

and

$$\frac{K^2}{4}[V_{ab}^2]_{\mathrm{av}}=0.0009\ \mathrm{MHz}^2\ .$$

Both quantities are small compared to the corresponding ones determined above for the $Na_xK_{1-x}CN$ system. The ratios $[V_{ab}^2]_{\mathrm{av}}/[V_{aa}^2]_{\mathrm{av}}$, however, are of the same order of magnitude.

Clearly, Eq. (13) (see Fig. 5) provides a much more accurate determination of the second moments of the EFG distributions than an inspection of the shape of the central line used previously[24] for the case of the $Na(CN)_xCl_{1-x}$ system. For this reason, we did not quantitatively analyze the central line spectra presented in Fig. 3 for the $Na_xK_{1-x}CN$ system.

Since $[V_{aa}^2]_{\mathrm{av}}$ and $[V_{ab}^2]_{\mathrm{av}}$ measure the mean deviations from cubic symmetry according to (13), this statement holds for the second moment $M_2^{(1)}$, too. It, thus, should be sensitive to a random orientational freeze-out of the CN quadrupoles. We therefore measured the temperature dependence of the second moments of the satellite distributions. The determination of $M_2^{(1)}$ is rather simple as long as the satellite frequency distributions have a Gaussian shape. This case applies to all temperatures investigated so far in the $Na(CN)_xCl_{1-x}$ system (above about 80 K) and to temperatures above about 200 K in the $Na_xK_{1-x}CN$ system.

In Figs. 6 and 7 we present the temperature dependences of the second moments of the ^{23}Na satellite distributions in the $Na(CN)_xCl_{1-x}$ system and the $Na_xK_{1-x}CN$ system, respectively, in the temperature region where the distributions are Gaussian. In addition, in Fig. 6, second moment data of the ^{35}Cl central lines in the $Na(CN)_xCl_{1-x}$ system are shown. The widths of the distributions increase considerably and continuously on lowering the temperature. This reflects the drastic and continuous change of the local environments which, because of the average cubic structure, can be attributed to the occurrence of preferential directions for the orientations of the CN molecules and can be identified with the establishment of the quadrupolar glass state. For the $Na(CN)_xCl_{1-x}$ system, the anomalous temperature dependence starts at about 200 K, whereas for the other system it starts at about 400 K. The widths of the satellite frequency distributions are at low temperatures comparable to the ^{23}Na satellite line splitting observed in the low-temperature phase of pure NaCN.[39] In the $Na_xK_{1-x}CN$ system in the concentration range under investigation, the ^{23}Na satellite distributions are at the same temperature considerably broader than in $Na(CN)_{0.65}Cl_{0.35}$ (i.e., $x \approx x_c$). Moreover, a characteristic concentration dependence is observed for the $Na_xK_{1-x}CN$ system indicating the broadest distribution to occur at $x \approx 0.5$. This contrasts to the behavior of the $Na(CN)_xCl_{1-x}$ system (Fig. 6) where a monotonic dependence of the distribution width of the ^{35}Cl central line on x is observed. T_1 measurements,[24,31] moreover, confirm that, in this temperature range, the fast motion regime is

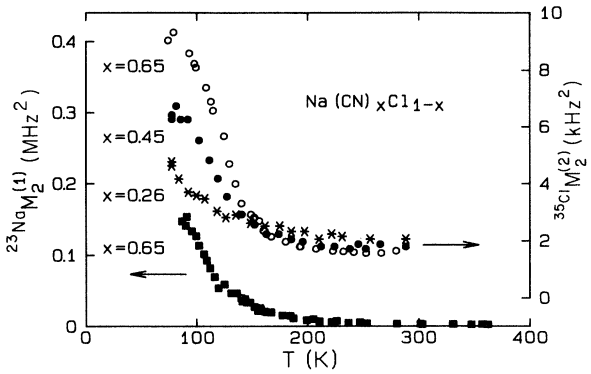

FIG. 6. Temperature dependences of the second moments M_2 of the ^{23}Na satellite distributions and the ^{35}Cl central lines in the $Na(CN)_xCl_{1-x}$ system for $\mathbf{B}_0\|[110]$. (The ^{35}Cl second moments were estimated from the full width at half-height.)

realized, i.e., the observed increase of the distribution widths should be ascribed to an orientational freeze-out of the CN ions and not to a mere motional-narrowing effect.

On lowering the temperature, in the $Na_xK_{1-x}CN$ system, characteristic shoulders occur in the spectra. This effect can be observed for the satellite distribution (Fig. 8) as well as for the central line (Fig. 9). Figure 10 shows for another concentration $x=0.57$ how the spectra of the ^{23}Na satellite lines gradually broaden and the shoulders emerge on lowering the temperature. Obviously, the assumptions on which the central limit theorem is based are no longer fulfilled and the preferential orientations of the CN quadrupoles show up directly in the measured spectra. In the $Na(CN)_{0.65}Cl_{0.35}$ system even at low temperatures no such shoulders could be detected. As long as an exact microscopic theory for the satellite spectra in the temperature regime where the shoulders occur is not available, the second moment cannot be reliably determined from the experimental data because the high- and

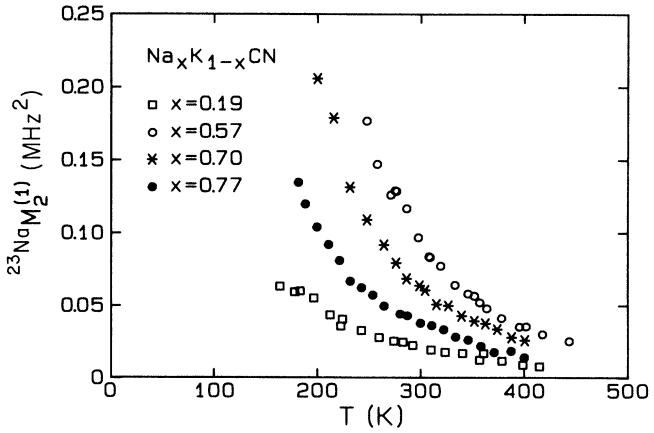

FIG. 7. Temperature dependences of the second moments $M_2^{(1)}$ of the ^{23}Na satellite distributions in the $Na_xK_{1-x}CN$ system for $\mathbf{B}_0\|[110]$, for the temperature region where Gaussian distributions are present.

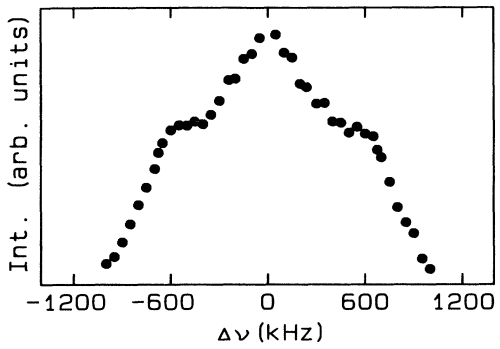

FIG. 8. Distribution of ^{23}Na satellite lines for a $Na_{0.7}K_{0.3}CN$ crystal and $\mathbf{B}_0 \| [110]$ at $T = 141$ K [compare to Fig. 4(a)].

low-frequency tails of the spectra which contribute considerably to $M_2^{(1)}$ are not known.

It has been mentioned above that, at ambient temperature, the shape of the ^{23}Na central line in $Na_xK_{1-x}CN$ contains, for $\mathbf{B}_0 \| [100]$, only shifts to higher frequencies. According to Fig. 9, this result is retained on lowering the temperature, i.e., it can also be confirmed for the case that the shoulders are present. The same statement holds for the concentrations $x = 0.57$ and 0.77 investigated.

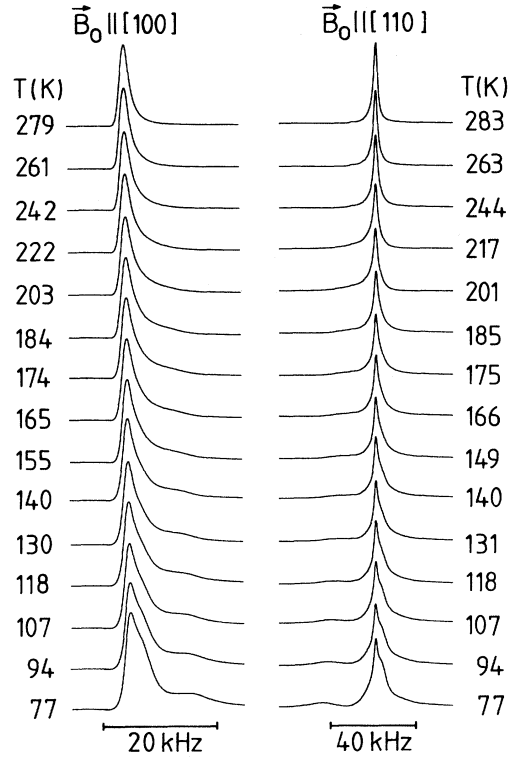

FIG. 9. Temperature dependence of the shape of the ^{23}Na central line for a $Na_{0.7}K_{0.3}CN$ crystal as measured at $\nu_L = 79.4$ MHz and the crystal orientations indicated by Fourier transforming the FID. The spectra are normalized. Analogous results have been obtained for $x = 0.57$ and 0.77.

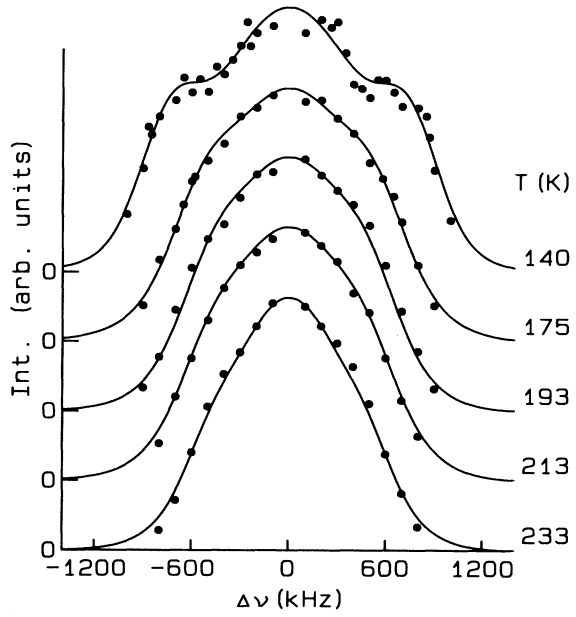

FIG. 10. Distributions of ^{23}Na satellite lines for a $Na_{0.57}K_{0.43}CN$ crystal at the temperatures indicated and $\mathbf{B}_0 \| [110]$. The curves given are guides to the eye and no fits.

With the aid of (2), it is therefore concluded that, in the whole temperature range for crystals which do not undergo a phase transition, the distribution functions of the EFG obey the condition $[V_{ab}^2]_{av} = 0$. This means that the principal axes of the EFG at each sodium nucleus continue to be directed along the cubic directions. The same statement has been derived previously[24] for the $Na(CN)_xCl_{1-x}$ system.

According to symmetry arguments applied to the $Na_xK_{1-x}CN$ system, the sodium-potassium disorder cannot account for the fact that the principal axes of the EFG at each sodium site are directed along the cubic axes. On the contrary, it has to be assumed that the CN dumbbells directly give rise to the main contribution to the EFG at the sodium sites. Thus, in both systems, $Na_xK_{1-x}CN$ and $Na(CN)_xCl_{1-x}$, the temperature dependence of the ^{23}Na EFG reflects the ordering process of the CN dumbbells.

Obviously, these symmetry properties of the EFG are related to the symmetry properties of the probability distribution of the orientations of the CN dumbbells. It may reasonably be assumed that the CN ions are essentially oriented in a way that their axes are parallel to the cubic directions. This can be justified by considering a multipole expansion of the nearest-neighbor contributions to the EFG at the sodium sites. The EFG's, due to the point charges of the neighboring anions, sum up to zero because of the cubic symmetry. The dipole moments of the CN ions can be disregarded not only because they are rather small, but mainly because the fast motions average out this contribution. The EFG which appears is thus essentially related to the quadrupole moments of the CN ions. If a quadrupole is oriented parallel to one of the cubic axes, the corresponding contribution to the EFG at a

neighboring Na site has, with symmetry arguments, its principal axes parallel to the cubic axes. This, then, also holds for a sum of such contributions. If, on the other hand, other preferred orientations for the CN quadrupoles are assumed, in contradiction with the experiments, arbitrary orientations of the EFG principal axes are expected.

Results derived for the probability distributions of the orientations of the CN molecules in different mixed alkali cyanides by different experimental methods seem to support our supposition concerning the preferred orientations of the CN dumbbells: In pure NaCN (Ref. 40) (single-crystal neutron diffraction) and in the very diluted case NaCl:CN (Ref. 41) (investigation of the birefringence and Kerr effect), the CN dumbbells have their maximum orientational probability along the [100] directions. Pure KCN (Ref. 40) and KCl:CN,[41] on the contrary, show maximum probability for the CN molecules along the [111] directions. Single-crystal neutron-diffraction studies in $K(CN)_xBr_{1-x}$ (Ref. 42) yielded favored alignments of the CN molecules along the [100] directions with decreasing temperature. Particularly in $K(CN)_{0.53}Br_{0.47}$, for temperatures $T \lesssim 140$ K, the CN ions are aligned with highest probability along [100]; at higher temperatures the maximum probability for the CN orientations is along [111].[42] Recent single-crystal ^{15}N NMR studies[43] in the same system $K(CN)_xBr_{1-x}$ show, for $x=0.50$ and 0.20 at low temperatures, preferred alignment along [100] directions. According to this work, the orientation distribution function has its maximum along [100] directions, is intermediate in [110] directions, and is nearly zero along [111] axes. Both experimental results disagree with molecular-dynamics simulations[44] that find strong [111] preferential alignment. For the $Na_xK_{1-x}CN$ system with $x=0.81$, 0.56, and 0.11 single-crystal neutron-diffraction studies[10] give—even at ambient temperature—the most probable orientation of the CN ions again along the [100] directions. Especially, for $x=0.81$ and 0.56, the probability for deviations from these orientations is rather small. With decreasing temperature, the preference of the [100] directions is even enhanced.[10]

Thus, the central assumption that the CN ions are oriented parallel to the cubic directions obviously explains the symmetry properties of the EFG. It should be stressed, however, that it is in conflict with the assumptions introduced usually to account for the considerable softening of the elastic shear modulus c_{44}. A detailed discussion of the problems related to this topic will be given below in Sec. VI.

As for the alkali cyanide halide mixed systems,[45] pronounced effects of phase transitions on the NMR line distributions are expected for the $Na_xK_{1-x}CN$ mixed systems which still undergo a phase transition. Corresponding results are presented in Figs. 11 and 12. According to Fig. 11, the width of the ^{23}Na central line (in the system $x=0.92$) is, above T_c, comparatively small and shows a weak temperature dependence. Below T_c, a steep increase occurs and a saturation plateau is reached. For the sample showing a transition to the glass state ($x=0.70$), on the other hand, a continuous increase of

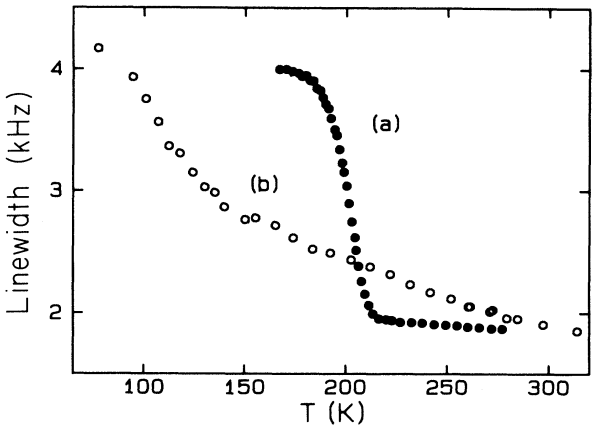

FIG. 11. Temperature dependence of the width of the ^{23}Na central line (at half-height) in $Na_xK_{1-x}CN$ for (a) $x=0.92$ and (b) $x=0.70$ and the crystal orientation $\mathbf{B}_0 \| [110]$.

the distribution width occurs at decreasing temperature. The values obtained for the linewidth at low temperatures exceed those obtained for $x=0.92$, thus indicating that the mean deviations from the local cubic symmetry of a ^{23}Na nucleus are larger in the former system. This effect is expected because the sodium-potassium disorder will presumably have the most pronounced local effect near $x=0.5$. Thus, Fig. 11 demonstrates that the behav-

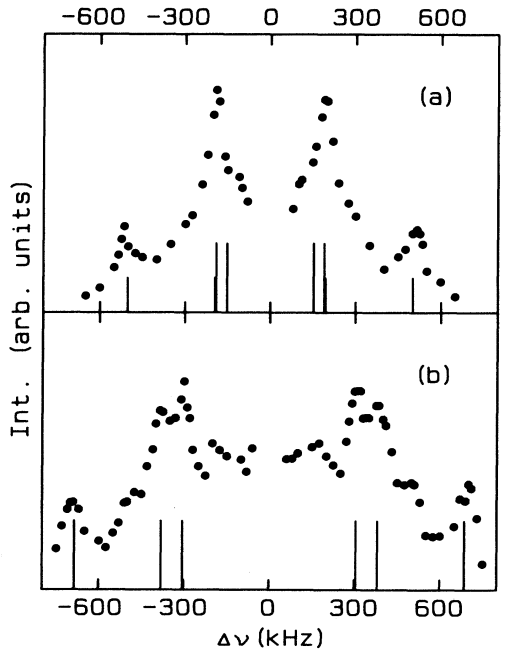

FIG. 12. Distributions of the ^{23}Na satellite lines for a $Na_{0.95}K_{0.05}CN$ crystal at $T=246$ K (just below T_c). The crystal orientations (a) $\mathbf{B}_0 \| [110]$ and (b) $\mathbf{B}_0 \| [100]$ are specified according to the high-temperature phase cubic reference frame. The lines indicate the frequencies and relative intensities of the ^{23}Na satellite lines observed in a multidomain sample of pure NaCN just below the phase transition (Ref. 39).

ior of systems which show no phase transition differs qualitatively from that of systems which still undergo a phase transition. The data, however, should not be overinterpreted because only a semiquantitative measure for the linewidth is given, which, e.g., does not account for shoulders.

According to Fig. 12, distinct centers of intensity show up in wide distributions of satellite lines. As expected, in both orientations the centers of intensity occur at frequencies where, for a multidomain sample of pure NaCN at the same orientation in the low-temperature phase, the satellite lines occur.[39] Moreover, the intensities concentrated in the distributions near these centers of intensity closely resemble the intensities of the ^{23}Na satellite lines of pure NaCN measured in the low-temperature phase at a multidomain sample in the orientations indicated.[39]

V. THEORETICAL MODEL

A. Definition of order parameters

The CN dumbbell represents an elastic quadrupole which can be described by a symmetric traceless Cartesian quadrupole tensor of rank 2 and dimension 3. With regard to the orientational freeze-out at low temperatures in the mixed cyanides, it will be convenient to replace the five independent components of the quadrupole tensor by the five orientational coordinates Y^α ($\alpha=1,2,\ldots,5$), the symmetry-adapted spherical harmonics of angular-momentum quantum number $1=2$.[5] For $\alpha=1$ and 2, the Y^α have E_g symmetry and are proportional to $3z^2-1$ and x^2-y^2, whereas for $\alpha=3$, 4, and 5, they have T_{2g} symmetry and are proportional to xy, yz, and zx, respectively.[5] [Here we used Cartesian coordinates; $\mathbf{u}=(x,y,z)$ is the unit vector along the C—N bond.]

The Hamiltonian for a set of elastic quadrupoles with randomly quenched and frustrated pairwise interactions[12] can be expressed now for the mixed cyanides[19–21,46] in terms of these symmetry-adapted spherical harmonics Y^α as

$$\mathcal{H}=-\sum_{i,j}\sum_{\alpha,\alpha'=1}^{5} J_{ij}^{\alpha,\alpha'} Y_i^\alpha Y_j^{\alpha'} - \sum_i \sum_{\alpha=1}^{5} f_i^\alpha Y_i^\alpha \,. \tag{17}$$

Here the Y_i^α are the five orientational coordinates at site i. The f_i^α represent the random strain fields at site i and the coupling constants $J_{ij}^{\alpha,\alpha'}$ account for both the direct and the lattice-mediated[19–21] CN-CN quadrupole interactions. The lattice coordinates have already been eliminated from the Hamiltonian (17).

Following the model of Sherrington-Kirkpatrick[15] for magnetic spin glasses, the random interactions (or random bonds) J_{ij} and the random strain fields f_i are assumed to be independently distributed according to Gaussian probability densities:

$$P(J_{ij})=\left[\frac{N}{2\pi J^2}\right]^{1/2}\exp\left[-\frac{(J_{ij}-J_0/N)^2}{2J^2/N}\right], \tag{18}$$

$$P(f_i)=\left[\frac{1}{2\pi\Delta}\right]^{1/2}\exp[-f_i^2/(2\Delta)] \,, \tag{19}$$

with J_0, J, and Δ being concentration dependent, and N the number of quadrupoles. Extending the concepts for magnetic spin glasses to quadrupolar glasses, the quadrupolar Edwards-Anderson order parameter $q_{\rm EA}$ is defined here[12,13] as

$$q_{\rm EA}=\sum_\alpha q_\alpha \tag{20}$$

with

$$q_\alpha=[\langle Y_i^\alpha\rangle^2]_{\rm av}=\frac{1}{N}\sum_i \langle Y_i^\alpha\rangle^2 \,, \tag{21}$$

where $\langle\cdots\rangle$ represents the thermal average, while $[\cdots]_{\rm av}$ again denotes the disorder average, i.e., here the simultaneous average over random bonds and random fields. Equation (21) implies that q_α is self-averaging, i.e., the two types of averaging in (21) are fully equivalent.

In the high-temperature phase of the pure cyanides at each CN site, $\langle Y_i^\alpha\rangle=0$ ($\alpha=1,2,\ldots,5$) due to the fast reorientational motions of the CN dumbbells averaging out the molecular anisotropy. Thus, $[\langle Y_i^\alpha\rangle]_{\rm av}=0$ and $q_\alpha=[\langle Y_i^\alpha\rangle^2]_{\rm av}=0$. For a given domain in the orthorhombic phase of both the pure and the mixed cyanides, $[\langle Y_i^\alpha\rangle]_{\rm av}\neq 0$ for one Y^α of T_{2g} symmetry.[21] The monoclinic and rhombohedral phases, on the other hand, are characterized[21] by the condensation of two, respectively, three $[\langle Y_i^\alpha\rangle]_{\rm av}\neq 0$ ($\alpha=3,4,5$). In the quadrupolar glass phase, $[\langle Y_i^\alpha\rangle]_{\rm av}=0$ ($\alpha=1,2,\ldots,5$); the quadrupolar Edwards-Anderson order parameter $q_{\rm EA}$, however, is nonzero.

The probability distribution functions G_α of the mean local orientational coordinates $\langle Y_i^\alpha\rangle$ are defined as

$$G_\alpha(p_\alpha)=\frac{1}{N}\sum_i \delta(p_\alpha-\langle Y_i^\alpha\rangle)=[\delta(p_\alpha-\langle Y_i^\alpha\rangle)]_{\rm av} \,. \tag{22}$$

The first moment of this distribution $G_\alpha(p_\alpha)$ equals $[\langle Y_i^\alpha\rangle]_{\rm av}$, which vanishes in the quadrupolar glass phase. The second moment is just the order parameter

$$q_\alpha=\int p_\alpha^2 G_\alpha(p_\alpha)dp_\alpha \,. \tag{23}$$

In the quadrupolar glass phase of the mixed cyanides, the structure is cubic on the average down to lowest temperatures. Due to this symmetry, $q_1=q_2$ and $q_3=q_4=q_5$; i.e., only two different order parameters are involved.

B. Relation between $q_{\rm EA}$ and the second moment $M_2^{(1)}$

As we have seen, according to Eq. (13), the second moment $M_2^{(1)}$ of the ^{23}Na satellite distributions is a linear combination of $[V_{aa}^2]_{\rm av}$ and $[V_{ab}^2]_{\rm av}$. These EFG tensor components occurring at different nuclei in the mixed cyanides can, in principle, now be related to the ordering of the CN quadrupoles or, equivalently, to the functions Y^α describing the orientations of the dumbbells. Before discussing the "nonlocal case" realized for the ^{23}Na nuclei, we will start with the "local case" realized for the ^{14}N nuclei located in the CN dumbbell.

For a ^{14}N nucleus ($I=1$) located in the ith CN dumbbell, the spectrum of the NMR lines consists, in

first-order perturbation calculation, of two satellite lines ($m=\pm1\leftrightarrow m=0$) shifted from the unperturbed Larmor frequency ν_L by the same amount $\nu_i^{(1)}$ to higher and lower frequencies.[37] In analogy to Eq.(1), $\nu_i^{(1)}$ is also, in this case, proportional to the EFG component V_{zz}^i at the site of the ^{14}N nucleus. In analogy to the considerations in Sec. III, for the second moment $M_2^{(1)}$ of the ^{14}N satellite lines distribution equation (13) holds where the prefactor $\frac{1}{4}$ has to be replaced by $\frac{9}{16}$.

The term "local case" refers to the fact that the EFG at the ^{14}N nucleus is predominantly determined by the electronic configuration of the CN molecule. Thus, the EFG components V_{mn}^i in the cubic crystal reference frame ($m,n=a,b,c$) at a ^{14}N nucleus located in a certain CN molecule are completely determined by the orientations $\langle Y_i^\alpha \rangle$ of this dumbbell, i.e.,

$$V_{mn}^i = \sum_\alpha A_{i,\alpha}^{mn} \langle Y_i^\alpha \rangle \ . \tag{24}$$

This relation holds as long as the system is in the fast-motion regime. Accordingly, we have to calculate the second moments of the EFG tensor components in Eq. (24):

$$[(V_{mn}^i)^2]_{\rm av} = \sum_{\alpha,\alpha'} [A_{i,\alpha}^{mn} A_{i,\alpha'}^{mn} \langle Y_i^\alpha \rangle \langle Y_i^{\alpha'} \rangle]_{\rm av} \ . \tag{25}$$

Since the coefficients $A_{i,\alpha}^{mn}$ are independent of the site index i and the crystal structure is cubic on the average, the remaining average is simply[19]

$$[\langle Y_i^\alpha \rangle \langle Y_i^{\alpha'} \rangle]_{\rm av} = \delta_{\alpha\alpha'} [\langle Y_i^\alpha \rangle^2]_{\rm av} = \delta_{\alpha\alpha'} q_\alpha \ . \tag{26}$$

It follows that

$$[V_{mn}^2]_{\rm av} = \sum_\alpha A_\alpha^{mn} q_\alpha \tag{27}$$

with $A_\alpha^{mn} = (A_{i,\alpha}^{mn})^2$. Thus, the second moment of the ^{14}N satellite distribution is a linear combination of the order parameters q_α.

For the ^{23}Na as well as the ^{35}Cl and ^{39}K nuclei, we deal with the "nonlocal case" because they are located at positions other than in the CN quadrupole. Therefore, the EFG components V_{mn}^i (cubic crystal reference frame) at a given nucleus are (in principle) determined by the orientations of all CN quadrupoles in the crystal

$$V_{mn}^i = \sum_j \sum_\alpha B_{j,\alpha}^{i,mn} \langle Y_j^\alpha \rangle \ . \tag{28}$$

Here, the fast-motion case is again supposed. The second moment of the EFG tensor components can again be calculated:

$$[(V_{mn}^i)^2]_{\rm av} = \sum_{j,j'} \sum_{\alpha,\alpha'} [B_{j,\alpha}^{i,mn} B_{j',\alpha'}^{i,mn} \langle Y_j^\alpha \rangle \langle Y_{j'}^{\alpha'} \rangle]_{\rm av} \ . \tag{29}$$

It may be assumed that the coefficients $B_{j,\alpha}^{i,mn}$ are independent of the site index i, and thus $B_{j,\alpha}^{i,mn}$ are no random variables. Neglecting correlations between the different CN ions, the remaining average reduces to[19,47]

$$[\langle Y_j^\alpha \rangle \langle Y_{j'}^{\alpha'} \rangle]_{\rm av} = \delta_{\alpha\alpha'} \delta_{jj'} q_\alpha \ . \tag{30}$$

Consequently,

$$[V_{mn}^2]_{\rm av} = \sum_\alpha B_\alpha^{mn} q_\alpha \ , \tag{31}$$

where $B_\alpha^{mn} = \sum_j (B_{j,\alpha}^{i,mn})^2$, and, again, the second moment of the satellite distribution is a linear combination of the order parameters q_α.

All above considerations are valid if the local fluctuations of the quadrupoles are fast compared to the rigid lattice quadrupolar splittings. In the slow-motion regime, the additional broadening due to the slowing down of these fluctuations has to be taken into account. Consequently, the order parameter $q_{\rm EA}$ will saturate when the slow-motion regime is reached.

As already mentioned, due to the average cubic structure, only the two order parameters q_1 and q_3 are involved in the mixed cyanides. It has been shown in Sec. IV that the above result $[V_{ab}^2]_{\rm av}=0$ strongly suggests that we assume that the CN dumbbells are aligned along the cubic [100] directions. Consequently, the order parameter q_3, which measures deviations of the orientations of the CN dumbbells from the [100] directions, is small compared to q_1. Thus, the data will be interpreted in the following on the assumption that q_3 can be neglected and only one order parameter $q_1 \propto q_{\rm EA}$ is dominating in the mixed cyanides.

VI. DETERMINATION OF THE QUADRUPOLAR ORDER PARAMETER $q_{\rm EA}$

According to Eqs. (13) and (31) and the fact that $q_1 \propto q_{\rm EA}$, an experimental determination of the temperature dependence of the second moment $M_2^{(1)}$ of the satellite distributions yields the temperature dependence of $q_{\rm EA}$. The shape of the $q_{\rm EA}(T)$ curves should then allow a discrimination between a random-field-type single-ion freezing and a collective glass transition. Consequently, the ^{23}Na second moment data can be analyzed by

$$^{23\rm Na}M_2^{(1)} = A + Bq_{\rm EA}(T) \ . \tag{32}$$

For the second moments $M_2^{(2)}$ of the central lines, no corresponding exact relations are available. Nevertheless, the ^{35}Cl central line second moment data can be expanded for small $q_{\rm EA}$, i.e., sufficiently high temperatures, as

$$^{35\rm Cl}M_2^{(2)} = A' + B' q_{\rm EA}(T) \ . \tag{33}$$

Here A, A' describe the direct quadrupolar effect of static substitutional disorder and the residual dipolar width, whereas B, B' describe the effect of the orientational freeze-out. Accordingly, the results presented in Figs. 6 and 7 directly reflect the temperature dependences of the quadrupolar Edwards-Anderson order parameter $q_{\rm EA}$ in the various systems.

Since a calculation of $q_{\rm EA}$ for the presented quadrupolar glass model does not exist and since a continuous reorientation model,[19–21] a three-site model,[7,24] and even a two-site model[48] give qualitatively similar results in the high-temperature region, we tried as a first attempt to fit $q_{\rm EA}(T)$ with the random-bond–random-field Ising model:[48–50]

$$\mathcal{H} = -\sum_{i,j} J_{ij} S_i S_j - \sum_i (f_i + E) S_i \ . \tag{34}$$

Here $S=\pm 1$ is the pseudospin variable and E is a uniform external field. The random interactions J_{ij} and the random fields f_i are distributed according to Eqs. (18) and (19).

The normalized order parameters $p=[\langle S_i\rangle]_{\rm av}$ and $q_{\rm EA}=[\langle S_i\rangle^2]_{\rm av}$ are then determined by the coupled self-consistent equations:[48–50]

$$p=(2\pi)^{-1/2}\int dz\,\exp(-z^2/2)\times\tanh\{\beta[J(q_{\rm EA}+\Delta/J^2)^{1/2}z+J_0p+E]\}\ , \tag{35a}$$

$$q_{\rm EA}=(2\pi)^{-1/2}\int dz\,\exp(-z^2/2)\times\tanh^2\{\beta[J(q_{\rm EA}+\Delta/J^2)^{1/2}z+J_0p+E]\}\ , \tag{35b}$$

where $\beta=1/(k_BT)$ and, by analogy to Eqs. (18) and (19), J^2 is the variance of the random interactions and Δ the variance of the random fields. The glass phase is characterized by the solution $p=0$ and $q_{\rm EA}\neq 0$. For $\Delta=J=0$, Eqs. (35) reduce to the well-known molecular-field relation $p=\tanh[\beta(J_0p+E)]$ and $q_{\rm EA}=p^2$.

Our data in Figs. 6 and 7 were fitted with the aid of (32) and (33) to Eq. (35b). The results obtained for the quadrupolar Edwards-Anderson order parameter $q_{\rm EA}(T)$ are presented in Figs. 13 and 14.

No satisfactory fit could be obtained for the pure random-field-type single-ion freezing model (i.e., $J^2=0$) for any value of the random strain field variance Δ (Fig. 13, curves *a*, *b*, and *c*). Here all interactions between the CN quadrupoles are neglected and the CN ions reorient in temperature-independent potentials. We note that all models mentioned above give rise to the same high-temperature tail $q_{\rm EA}\propto\Delta/T^2$ but cannot account for both the tail and the observed curvature of the $q_{\rm EA}$ versus T plot.

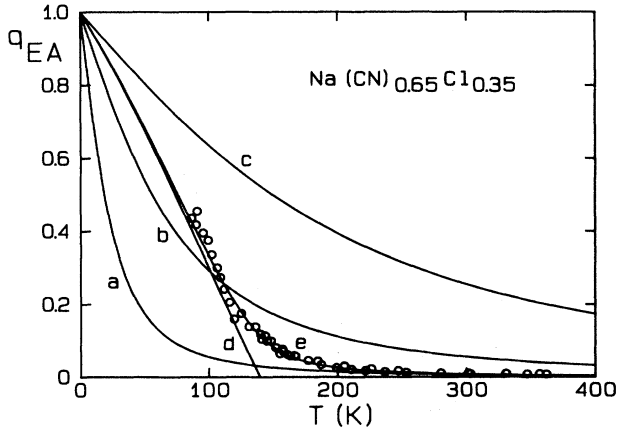

FIG. 13. Comparison between the temperature dependences of the quadrupolar Edwards-Anderson order parameter $q_{\rm EA}$ determined from the ^{23}Na satellite distribution's second moment $M_2^{(1)}$ data (Fig. 6) for the $Na(CN)_{0.65}Cl_{0.35}$ system (circles) and the predictions of the theoretical models. Curves *a*, *b*, and *c*: Pure random-field models ($J^2=0$) with $\Delta^{1/2}/k_B=25$, 75, and 200 K, respectively. Curve *d*: Pure random-bond model ($\Delta=0$) with $J/k_B=140$ K. Curve *e*: Fit to the random-bond–random-field model with $J/k_B=140$ K and $\Delta/J^2=0.03$.

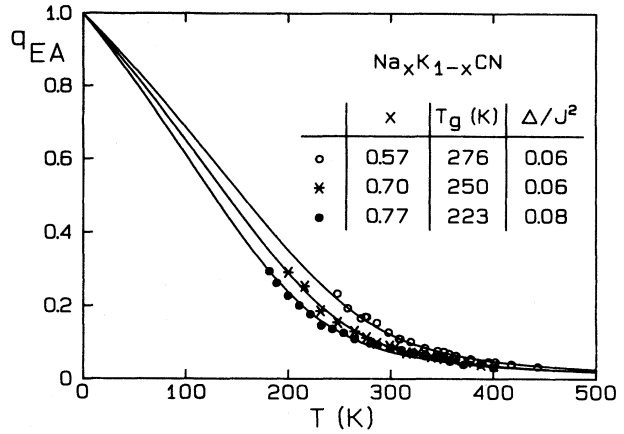

FIG. 14. Temperature dependences of the quadrupolar Edwards-Anderson order parameters determined from the ^{23}Na satellite distribution's second moment $M_2^{(1)}$ data (Fig. 7) for the $Na_xK_{1-x}CN$ system. The curves are the fits to the random-bond–random-field model with the parameters indicated.

We therefore turned to the collective model ($J^2\neq 0$) involving a glass transition. Also, no fit could be obtained for the pure collective model with $\Delta=0$, i.e., for random bonds without random fields (Fig. 13, curve *d*). Since the obtained $q_{\rm EA}$ values are already nonzero far above the nominal glass transition temperature $T_g=J/k_B$, we clearly do not deal with a classical random-bond-type glass transition with a sharp T_g with $q_{\rm EA}=0$ above T_g and $q_{\rm EA}\neq 0$ below T_g. Rather, the data indicate a random-field smearing of the quadrupolar glass transition, i.e., they require both J^2 and Δ to be nonzero. Here the random-field variance Δ induces a nonzero value of $q_{\rm EA}$ already far above T_g.

The agreement (Fig. 13, curve *e*) is surprisingly good. For the $Na(CN)_xCl_{1-x}$ system with $x=0.65$, we find $T_g=J/k_B=140$ K and a rather small value $\Delta/J^2=0.03$. The consistency of the results is moreover verified by the fact that the same $q_{\rm EA}$ values are also obtained from the ^{35}Cl data for the same sample. The ^{35}Cl data for $x=0.45$ (Fig. 6) can now be fitted with the same value of Δ/J^2 and $T_g=146$ K. This is exactly what is expected if the system behaves as an ideal solution so that $\Delta\propto x(1-x)$ and $J\propto[x(1-x)]^{1/2}$.[48] Very good fits can also be obtained for the $Na_xK_{1-x}CN$ data (Fig. 14) with the parameters indicated. As expected, Δ/J^2 is nearly concentration independent, but the value is larger than in the $Na(CN)_xCl_{1-x}$ system. Thus, the ^{23}Na as well as the ^{35}Cl quadrupolar perturbed NMR data clearly demonstrate that we deal in the mixed cyanides with a random-field smearing of a random-bond-type quadrupolar glass transition and not with a random-field-type "single-ion" freezing or a classical spin-glass-like glass transition.

VII. DISCUSSION AND COMPARISON

In this section our NMR results will be discussed in relation to those obtained from other methods. In previous works,[7,30] it was demonstrated that the widths of the ^{23}Na NMR satellite line distributions observed in $Na(CN)_{0.65}Cl_{0.35}$, i.e., in a system with a concentration near the critical one, and the widths of the cubic Bragg peaks show the same temperature dependence. It, therefore, can be taken for granted that the ^{23}Na NMR results presented here and previously,[24] for the two systems under consideration, give the correct onset of the freezing process and, moreover, to some extent, quantitatively the temperature dependence of the Edwards-Anderson order parameter.

The considerable softening and successive hardening, which, at least near the critical concentration x_c, is observed for the elastic shear stiffness c_{44},[7,25–29] seems to be the most striking property of the mixed alkali cyanides. It is therefore worthwhile discussing the relation between the behavior of the distributions of the NMR frequencies and the elastic stiffness c_{44} in more detail. For that purpose, we first discuss the current conceptions for describing the anomalous elastic behavior of the mixed alkali cyanides in a general context. In particular, we will extend the concepts and results developed by Fossum *et al.*[25] to the case of the random-bond–random-field model discussed previously.[48–50]

The behavior of c_{44} in the mixed cyanides has been explained in theoretical models by a bilinear coupling of the orientational degrees of freedom of the CN dumbbells to the translational lattice modes including random fields.[19–21] In this approach, the static elastic shear constant c_{44} is given by[19,25]

$$c_{44}=c_{44}^{0}\frac{T-T_c(1-q_{EA})}{T-T_0(1-q_{EA})}\ , \tag{36}$$

where c_{44}^{0} is the bare elastic constant. T_c is the ferroelastic ordering temperature in the absence of random strains and T_0 is an effective temperature at which the CN dumbbells would achieve quadrupolar order in the absence of bilinear coupling. For the mixed alkali cyanides, T_0 usually is negative and used as a fit parameter. According to (36), the hardening of c_{44} below the temperature of the minimum of c_{44} is due to the increase of q_{EA}. Note, however, that q_{EA} influences c_{44} according to (36) in a complex manner.

Following Michel,[19] Eq. (36) is only justified in a high-temperature expansion for which $q_{EA}\ll 1$, resulting in $q_{EA}\simeq\Delta/(k_BT)^2$, where, as above, Δ is the variance of the random-field distribution. Many authors (see Refs. 25–27 and 30 and works cited within) used Eq. (36) in the high-temperature expansion to fit the temperature dependences of the $c_{44}(T)$ curves for temperatures above the c_{44} minimum in different cyanide mixed systems, thus getting parameters $c_{44}^{0}(x)$, $T_c(x)$, $T_0(x)$, and $\Delta(x)$ depending on the concentration x. A problem arises if this high-temperature expansion is applied to lower temperatures, although the approximation $q_{EA}\ll 1$ breaks down in this temperature range. Nevertheless, Hu *et al.*[27] derived on that basis from their c_{44} data $\Delta/k_B^2=4690$ K^2 for the system $Na_{0.56}K_{0.44}CN$ which fits reasonably to $\Delta/k_B^2=4570$ K^2 derived above for $Na_{0.57}K_{0.43}CN$ from the NMR data. For other concentrations, however, larger differences occur. In addition, a joint fit of the $c_{44}(T)$ curves was achieved[25,28] by using the high-temperature expansion above the c_{44} minimum together with a phenomenological low-temperature expansion $q_{EA}\simeq 1-A_1T-A_2T^3$ below the minimum. The latter was proposed for random-field systems.[25,51] This procedure seems to be rather questionable since Eq. (36) is confirmed only for the high-temperature case and, moreover, the simultaneous application of both approximations near the minimum of c_{44} gives rise to considerable errors. (Note that $A_1>0$ and $A_2<0$ hold for Gaussian distributions of random fields,[51] whereas, in Refs. 25 and 28, a positive fit parameter A_2 was used.)

We now discuss to what extent the random-bond–random-field Ising model, which we used to fit our NMR results, can account for the behavior of $c_{44}(T)$. In a mean-field approach, a Landau expansion of the free energy generally yields

$$c_{44}=c_{44}^{0}(1-\gamma^2\chi)\ , \tag{37}$$

where γ is the translation rotation coupling constant and χ is the order-parameter susceptibility. The noncritical temperature dependence of c_{44}^{0} will be disregarded in the following considerations because it was shown to be small.[25]

We have calculated $\chi=(\partial p/\partial E)|_{E=0}$ in the random-bond–random-field Ising model, using Eqs. (35) obtaining for any state with $p=0$ (glass or disordered state), the following exact relation[15]

$$\chi^{-1}=\frac{k_BT}{1-q_{EA}}-J_0\ , \tag{38}$$

where q_{EA} is the solution of (35b). Combining (37) and (38), Eq. (36) is derived with the parameters $T_0=J_0/k_B$ and $T_c=T_0+\gamma^2/k_B$. Thus, in the frame of this model, (36) is an exact result for which the glass order parameter q_{EA} can be calculated on the basis of (35b). According to (38), the elastic behavior is determined not only by the parameters determining q_{EA}, but also by the additional parameter J_0 which influences the elastic behavior strongly even in temperature regions where $q_{EA}\ll 1$.

According to (36), the general relation between the $c_{44}(T)$ data available from experiment and q_{EA}

$$\frac{1-q_{EA}}{T}=\frac{c_{44}^{0}-c_{44}(T)}{T_cc_{44}^{0}-T_0c_{44}(T)} \tag{39}$$

is comparatively complex and contains three adjustable parameters, i.e., c_{44}^{0}, T_c, and T_0. On the other hand, the corresponding relations (32) and (33) between q_{EA} and the NMR second moments are linear in q_{EA} and contain only two parameters. Thus, NMR may be assumed to be more convenient for determining the temperature dependence of the glass order parameter.

Continuing the discussion of the elastic behavior according to (36), the temperature at which the minimum

of c_{44} occurs, is given by the relation

$$\frac{1-q_{EA}}{T}=\frac{d(1-q_{EA})}{dT}\ , \tag{40}$$

which means that the tangent at the $1-q_{EA}$ versus T curve passes through the zero point of the temperature scale. From Figs. 13 and 14, it becomes obvious that the temperature for which (40) holds depends sensitively on the parameters Δ and J used in the model [note that J_0 does not occur in (40)]. In particular, it can be shown on the basis of (35b) that for $J=0$, i.e., for a pure random-field model,

$$\frac{1-q_{EA}}{T}-\frac{d(1-q_{EA})}{dT}$$
$$=\frac{1}{T}\int dz\, z^2\exp(-z^2/2)\cosh^{-2}(\Delta^{1/2}z/k_BT) \tag{41}$$

holds. The right-hand side of this equation is positive for $T>0$ and vanishes for $T=0$. Consequently, a c_{44} minimum exists for $T=0$ and, with the aid of (36), it is concluded that $c_{44}(T)$ continuously increases with increasing T. Such a behavior was not observed for the mixed alkali cyanides and, consequently, a pure random-field model is inadequate.

We calculated the temperature dependence of $c_{44}(T)/c_{44}^0$ according to (36) by assuming various parameters T_c and T_0 and calculating q_{EA} from (35b). All these calculations clearly showed that the overall change of c_{44} between the minimum and $T=0$ is unreasonably small (this is not so if the high-temperature expansion of q_{EA} is used, which, near the minimum of c_{44}, is definitely not applicable). On the other hand, experiments clearly demonstrate[7,34] that, in contrast, there is a considerable increase of $c_{44}(T)$ below the minimum. This seems to indicate that the present approach, in particular Eq. (36), is not applicable for describing the elastic behavior completely.

The random-bond–random-field model discussed here indeed has the following main shortcomings.

(i) It is uniaxial and thus disregards the three-dimensional character of the glass transition in the mixed cyanides. In particular, three-dimensional clusters, which are likely to be of some relevance, are not taken into consideration.

(ii) Because of (35) and (38), it only accounts for transitions of second order. On the other hand, in the mixed cyanides, the macroscopic phase transitions are of first order, whereas the transitions to the glass state are continuous. Thus, at the critical concentrations, the first-order character of the phase transitions is lost, which is a typical feature of a tricritical point.

(iii) In this model, an Almeida-Thouless-type line exists in the temperature-random-field variance plane[48] separating the high-temperature ergodic pseudo-spin-glass phase characterized by a single order parameter $q=q_{EA}$ from the nonergodic low-temperature phase characterized[16] by an order-parameter function. Further investigations of the dynamic behavior are needed to check on this point.

The first point may be improved by considering a multiple axes reorientational order-disorder model with cubic symmetry. In a first approximation, a model where the CN dumbbells are assumed to reorient quickly between the cubic directions has previously been considered.[7,24] The central self-consistent relation for the glass order parameter of that model is a generalization of Eq. (35b). For the case of $Na(CN)_{0.65}Cl_{0.35}$, it could be shown by an argumentation similar to that given above that both random bonds and random fields are necessary for describing the experimental data. This confirms the above statement that the high-temperature approximation gives rise to the same temperature dependences in all models.

This model is still incomplete because it does not take into consideration anything other than the cubic directions for the orientations of the CN dumbbells. It is indeed in conflict with the usually employed theories explaining the strong softening of c_{44} by a bilinear coupling of the elastic translational lattice modes to the orientational degrees of freedom of the dumbbells. It is well known[29,52] that dumbbells with a [100] orientation in a cubic crystal couple only to $A_{1g}+E_g$ strains associated to longitudinal phonons propagating along [100]. Consequently, only the elastic modulus c_{11} is affected. This quantity, however, is known to be much less influenced than c_{44} by the ordering process in the mixed cyanides. An interaction with transverse phonons, which produce T_{2g} strains, and to which a shear elastic modulus c_{44} is ascribed, requires in cubic crystals orientations of the CN molecules along the [110] or [111] directions.[52] Thus, the dumbbells must also possess equilibrium orientations where they are not oriented along one of the cubic [100] directions.

For a solution of the second question, generalizations of Eq. (35) have to be derived, which on a phenomenological level describe both first-order and second-order transitions. It is well known that, for the description of phase transitions in homogeneous systems, this can be achieved by considering a phenomenological Landau equation of state. It can be derived from the Weiss molecular-field equation, which corresponds to Eq. (35) and which allows only phase transitions of second order, by introducing suitable additional terms in the order parameter. A corresponding formalism for disordered systems seems not to exist.

VIII. CONCLUDING REMARKS

We have shown that quadrupolar perturbed NMR can contribute considerably to an understanding of the quadrupolar glass state in the mixed cyanides $Na(CN)_xCl_{1-x}$ and $Na_xK_{1-x}CN$. At high enough temperatures, the EFG distributions at the ^{23}Na nuclei have a Gaussian shape in both types of systems. The widths of the distributions are narrow at high temperatures, whereas there is a considerable and continuous broadening with decreasing temperature, which, because the average structure remains cubic, has to be attributed to the random orientational freeze-out of the CN ions, i.e., to the establishment of the quadrupolar glass state. The qualitative understanding is the following: At high temperatures, the CN ions move in nearly cubic potentials regardless of the

distribution of ions in the respective surroundings. With decreasing temperature, the local potentials are deformed by local fields caused by collective CN-CN interactions ("random bonds") as well as by random strain fields, which are due to the compositional disorder.

In a quantitative approach, the Edwards-Anderson order parameter q_{EA} could be derived from the widths of the frequency distributions measured by NMR. Comparing to the predictions of theoretical models, it could be shown that neither pure "random-bond" nor pure "random-field" models are adequate. On the contrary, the NMR results can be explained by assuming a smearing of the quadrupolar glass transition by weak random fields.

The symmetry and orientational dependence of the ^{23}Na NMR spectra in the systems mentioned indicate that, in the entire temperature range investigated, the EFG at each sodium site is oriented in the way that its principal axes are directed along the axes of the mean cubic structure. For the $Na_xK_{1-x}CN$ system, this statement has been proved by inspecting the orientational dependence of the satellite spectra for $x=0.57$ and 0.70 at ambient temperature. For the $Na(CN)_{0.65}Cl_{0.35}$ system, it was shown by reevaluating the previous satellite data[24] for temperatures above about 160 K. For all other temperatures and concentrations, this statement is derived from the symmetry property of the central line in a crystal orientation where a cubic axis is parallel to the static magnetic field. Of course, in the latter case, a minor accuracy had to be accepted. Therefore, in these cases, too, investigations on the orientational dependence of the satellite distributions would be highly desirable. Despite these shortcomings, we are confident that the symmetry property of the EFG at the ^{23}Na site hold for the systems under investigations.

This symmetry property of the EFG is related to the possible orientations of the CN dumbbells. We have concluded that the CN molecules are oriented in both types of crystals with their axes parallel to the directions of the mean cubic structure. Other assumptions for the orientations of the dumbbells are in conflict with the symmetry of the EFG at the sodium site. On the other hand, other orientations are needed in order to be able to construct a bilinear coupling between the orientational degrees of freedom and the translational lattice modes, giving rise to the anomalous elastic behavior. Evidence for small-angle misorientations of the CN ions in the ordered orthorhombic phase of pure KCN from the orientations parallel to the orthorhombic b axis was observed in ^{13}C spin-lattice-relaxation measurements.[53] Corresponding small-angle deviations of the CN ions from the [100] directions in the mixed cyanides, which could explain the elastic behavior, cannot be excluded from our NMR results. Nevertheless, the solution of this conflict seems to be an important task for future investigations.

At low temperatures in the ^{23}Na spectra measured in the $Na_xK_{1-x}CN$ system, typical shoulders occur, i.e., strong deviations from the Gaussian distributions of EFG's. Except for the preliminary attempts described in Ref. 31, we have not carried out calculations to relate these measured spectra to the orientation distributions of the CN dumbbells and, in particular, to the glass order parameter.

ACKNOWLEDGMENTS

The authors are indebted to J. Albers and A. Klöpperpieper for growing and characterizing the crystals, to K. H. Michel for stimulating discussions, and to the Deutsche Forschungsgemeinschaft (Sonderforschungsbereich 130) for financial support.

*Permanent address: Hoechst AG, ZF II, Post-Box 800320, D-6230 Frankfurt/Main, Federal Republic of Germany.

[1]E. Courtens, J. Phys. (Paris) Lett. **43**, L199 (1982); Phys. Rev. Lett. **52**, 69 (1984); Jpn. J. Appl. Phys. Suppl. **24-2**, 70 (1985).

[2]R. Blinc, J. Dolinšek, R. Pirc, B. Tadić, B. Zalar, R. Kind, and O. Liechti, Phys. Rev. Lett. **63**, 2248 (1989).

[3]J. J. van der Klink, D. Rytz, F. Borsa, and U. T. Höchli, Phys. Rev. B **27**, 89 (1983); U. T. Höchli and M. Maglione, J. Phys.: Condens. Matter **1**, 2241 (1989).

[4]F. Lüty, in *Defects in Insulating Crystals,* edited by V. M. Turkevich and K. K. Shvarts (Springer-Verlag, Berlin, 1981), p. 69.

[5]K. H. Michel and J. M. Rowe, Phys. Rev. B **22**, 1417 (1980).

[6]K. Knorr, Phys. Scr. **T19**, 531 (1987).

[7]S. Elschner, J. Petersson, J. Albers, and J. K. Krüger, Ferroelectrics **78**, 43 (1988).

[8]F. Lüty and J. Ortiz-Lopez, Phys. Rev. Lett. **50**, 1289 (1983); J. Ortiz-Lopez and F. Lüty, Phys. Rev. B **37**, 5461 (1988).

[9]A. Loidl, T. Schräder, R. Böhmer, K. Knorr, J. K. Kjems, and R. Born, Phys. Rev. B **34**, 1238 (1986).

[10]T. Schräder, A. Loidl, and T. Vogt, Phys. Rev. B **39**, 6186 (1989); Z. Phys. B **79**, 423 (1990); T. Schräder, A. Loidl, G. J. McIntyre, and C. M. E. Zeyen, Phys. Rev. B **42**, 3711 (1990).

[11]A. Loidl, Annu. Rev. Phys. Chem. **40**, 29 (1989).

[12]H.-O. Carmesin and K. Binder, Z. Phys. B **68**, 375 (1987).

[13]P. M. Goldbart and D. Sherrington, J. Phys. C **18**, 1923 (1985).

[14]S. F. Edwards and P. W. Anderson, J. Phys. F **5**, 965 (1975); for a review on spin glasses, see K. Binder and A. P. Young, Rev. Mod. Phys. **58**, 801 (1986).

[15]D. Sherrington and S. Kirkpatrick, Phys. Rev. Lett. **35**, 1792 (1975).

[16]G. Parisi, Phys. Rev. Lett. **43**, 1754 (1979).

[17]R. Kree, L. A. Turski, and A. Zippelius, Phys. Rev. Lett. **58**, 1656 (1987).

[18]U. Bengtzelius, W. Götze, and A. Sjölander, J. Phys. C **17**, 5915 (1984).

[19]K. H. Michel, Phys. Rev. B **35**, 1405 (1987); **35**, 1414 (1987).

[20]C. Bostoen and K. H. Michel, Z. Phys. B **71**, 369 (1988).

[21]K. H. Michel and T. Theuns, Phys. Rev. B **40**, 5761 (1989).

[22]W. Rehwald, J. R. Sandercock, and M. Rossinelli, Phys. Status Solidi A **42**, 699 (1977).

[23]S. Elschner and J. Petersson, Z. Naturforsch. A **41**, 343 (1986).

[24]S. Elschner and J. Petersson, J. Phys. C **19**, 3373 (1986).

[25]J. O. Fossum and C. W. Garland, Phys. Rev. Lett. **60**, 592 (1988); J. O. Fossum, A. Wells, and C. W. Garland, Phys. Rev. B **38**, 412 (1988).
[26]C. W. Garland, J. O. Fossum, and A. Wells, Phys. Rev. B **38**, 5640 (1988).
[27]Z. Hu, C. W. Garland, and A. Wells, Phys. Rev. B **40**, 5757 (1989).
[28]J. Hessinger and K. Knorr, Phys. Rev. Lett. **63**, 2749 (1989).
[29]J. F. Berret and R. Feile, Z. Phys. B **80**, 203 (1990).
[30]S. Elschner, K. Knorr, and A. Loidl, Z. Phys. B **61**, 209 (1985).
[31]W. Wiotte, S. Elschner, and J. Albers, *Proceedings of the 23rd Congress Ampere, Rome (1986),* edited by B. Maraviglia, F. De Luca, and R. Campanella (Istituto Superiore di Sanitá, Rome, 1986), p. 142.
[32]K. Knorr, Solid State Ionics **39**, 91 (1990).
[33]S. Elschner, J. Albers, A. Loidl, and J. K. Kjems, Europhys. Lett. **4**, 1139 (1987).
[34]J. K. Krüger, R. Jiménez, K.-P. Bohn, J. Petersson, J. Albers, A. Klöpperpieper, E. Sauerland, and H. E. Müser, Phys. Rev. B **42**, 8537 (1990).
[35]R. Jiménez, K.-P. Bohn, J. K. Krüger, and J. Petersson, Ferroelectrics **106**, 175 (1990).
[36]M. H. Cohen and F. Reif, in *Solid State Physics,* edited by F. Seitz and D. Turnbull (Academic, New York, 1957), Vol. 5, p. 321.
[37]G. M. Volkoff, Can. J. Phys. **31**, 820 (1953).
[38]R. Kind, O. Liechti, R. Brüschweiler, J. Dolinšek, and R. Blinc, Phys. Rev. B **36**, 13 (1987); O. Liechti and R. Kind, J. Magn. Reson. **85**, 480 (1989).
[39]W. Buchheit, S. Elschner, H. D. Maier, J. Petersson, and E. Schneider, Solid State Commun. **38**, 665 (1981).
[40]J. M. Rowe and S. Susman, Phys. Rev. B **29**, 4727 (1984).
[41]A. Diaz-Gongora and F. Lüty, Phys. Status Solidi B **86**, 127 (1978).
[42]A. Loidl, K. Knorr, J. M. Rowe, and G. J. McIntyre, Phys. Rev. B **37**, 389 (1988).
[43]J. H. Walton and M. S. Conradi, Phys. Rev. B **41**, 6234 (1990).
[44]L. J. Lewis and M. L. Klein, J. Phys. Chem. **91**, 4990 (1987); Phys. Rev. B **40**, 7080 (1989).
[45]J. Albers, S. Elschner, A. Klöpperpieper, and J. Petersson, Ferroelectrics **55**, 101 (1984).
[46]A. P. Mayer and R. A. Cowley, J. Phys. C **21**, 4835 (1988).
[47]S. Elschner, Ph.D. thesis, University of Saarbrücken, 1986.
[48]R. Pirc, B. Tadić, and R. Blinc, Phys. Rev. B **36**, 8607 (1987).
[49]R. Blinc, J. Dolinšek, B. Zalar, A. Fuith, and H. Warhanek, Phys. Rev. B **40**, 10 753 (1989).
[50]R. Blinc, Z. Naturforsch. A **45**, 313 (1990).
[51]A. Aharony, Phys. Rev. B **18**, 3318 (1978).
[52]N. E. Byer and H. S. Sack, Phys. Rev. Lett. **17**, 72 (1966).
[53]H. T. Stokes, T. A. Case, and D. C. Ailion, Phys. Rev. Lett. **47**, 268 (1981); H. T. Stokes, D. C. Ailion, and T. A. Case, Phys. Rev. B **30**, 4925 (1984).